Development 124, 1033-1044 (1997)
Printed in Great Britain © The Company of Biologists Limited 1997
DEV4790

nodal expression in the primitive endoderm is required for specification of the anterior axis during mouse gastrulation

Isabelle Varlet, Jérôme Collignon† and Elizabeth J. Robertson*

Department of Molecular and Cellular Biology, Harvard University, 16 Divinity Avenue, Cambridge, MA 02138, USA

*Author for correspondence (e-mail: ejrobert@husc.harvard.edu)
†Present address: Department of Developmental Neurobiology, Guys Hospital, London SE1 9RT, UK

SUMMARY

Mouse nodal, a member of the TGFβ family of secreted growth factors is essential for gastrulation. We recently generated a *nodal*^{lacZ} reporter allele by homologous recombination in ES cells. In the present study, β-galactosidase staining in the perigastrulation-stage embryo has demonstrated the site of highest *nodal* expression is localised to the prospective posterior region of the epiblast marking the site of primitive streak formation. We also documented transient *nodal.lacZ* expression in the visceral endoderm prior to and during early streak formation. A mosaic analysis using wild-type ES cells to rescue *nodal*-deficient embryos allowed us to document functionally distinct nodal activities in the embryonic ectodermal and primitive endodermal cell lineages. nodal signaling in the ectoderm is necessary for primitive streak formation as the gastrulation defect of *nodal*-deficient embryos can be rescued by the inclusion of small numbers of wild-type cells. In addition, we show that chimeric embryos composed of *nodal*-deficient primitive endoderm fail to develop rostral neural structures. Thus we conclude that the action of nodal, a TGFβ-related growth factor expressed in the primitive endoderm, is critical for patterning of the anterior aspects of the A-P axis.

Key words: *nodal*, mouse gastrulation, primitive endoderm, chimeras

INTRODUCTION

Nodal, a member of the TGFβ family of secreted growth factors, was originally identified due to its close linkage with the 413.d proviral integration site (Zhou et al., 1993; Conlon et al., 1994). Homozygous *413.d* mutant embryos lacking *nodal* expression cannot initiate primitive streak formation and are arrested at the gastrulation stage of development (Conlon et al., 1991, 1994). The recent identification of conserved *nodal* homologs in *Xenopus* and chick (Smith et al., 1995; Jones et al., 1995) has underscored the key role played by the nodal signaling pathway during vertebrate development. Comparisons of the carboxyl-terminal signaling domains of *Xenopus*, chick and mouse nodal sequences indicate these molecules to share between 52 and 78% amino acid identity. Interestingly individual *Xenopus nodal* homologs seem to have distinct functional activities. For example, both *Xnr-1* and *Xnr-2* act as potent inducers of dorsal mesoderm cell types in manipulated frog embryos, and can also completely rescue UV-ventralized embryos (Jones et al., 1995). By contrast, *Xnr-3* lacks mesoderm-inducing activities per se, but rather appears to be required for cell migration and movement (Smith et al., 1995). On the other hand, several aspects of the nodal signaling pathway are highly conserved between higher and lower vertebrates. Recent studies demonstrate that the mouse *nodal* gene is transiently expressed in a discrete population of lateral plate mesoderm on the left side of the early somite-stage embryo, where its expression appears to be functionally correlated with the direction of axial rotation and the establishment of the definitive left-right (L/R) axis (Collignon et al., 1996; Lowe et al., 1996). Similarly both the chick *Cnr-1* (Levin et al., 1995) and *Xenopus Xnr-1* (Lowe et al., 1996) genes are asymmetrically expressed in left lateral mesoderm, suggesting a conserved molecular pathway determines the vertebrate L/R body axis.

nodal gene expression has been detected at the onset of gastrulation both by RT-PCR (Zhou et al., 1993) and in situ hybridization (Conlon et al., 1994). We recently used gene targeting techniques to introduce a *lacZ* reporter gene under control of the endogenous *cis*-regulatory elements into the mouse *nodal* locus (Collignon et al., 1996). The increased resolution afforded by β-gal staining has allowed us to precisely describe highly dynamic and transient *nodal* expression at early stages of mouse development. In the present study, we demonstrate that *nodal* is expressed throughout the epiblast tissue prior to overt streak formation, but becomes rapidly localized within the embryonic ectoderm to mark the future caudal region where the streak will form. Intriguingly, we find that *nodal* is also transiently expressed in the primitive endoderm cells overlying the embryonic ectoderm when gastrulation is initiated. Although the precise developmental role of the primitive endoderm in mammals has yet to be established, the equivalent cell lineage in chick, the hypoblast, is known to provide inductive signals influencing the position and

orientation of the primitive streak (Waddington, 1933; Azar and Eyal-Giladi, 1981).

Here we also analyse nodal signaling in the primitive endoderm during gastrulation and establishment of the anterior-posterior (A-P) axis. We have exploited the pronounced developmental bias of ES cells, which colonize almost exclusively derivatives of the embryonic ectoderm following re-introduction into blastocyst-stage embryos (Beddington and Robertson, 1989), to distinguish nodal activities in the embryonic ectoderm and the primitive endoderm lineages of the embryo. Our previous experiments demonstrated that *413.d* mutant ES cells injected into wild-type host blastocysts were capable of contributing to a wide variety of normal embryonic and adult tissue types in chimeras (Conlon et al., 1991). The present experiments show that very few wild-type epiblast cells are required to efficiently rescue the gastrulation defect of *413.d* mutant embryos, endorsing an essential role for the nodal signaling pathway in primitive streak initiation. However, we observe profound developmental defects in mosaic embryos in which the primitive endoderm lineage is composed exclusively of *nodal*-deficient cells. The rostral-most regions of the developing central nervous system (CNS) were consistently lacking in these embryos. These findings demonstrate an essential role for the primitive endoderm lineage in the establishment of anterior pattern during mouse gastrulation.

MATERIALS AND METHODS

Mouse strains and ES cells

The *nodal*^{lacZ} allele was maintained on a 129/Sv background and animals genotyped as described (Collignon et al., 1996). Mice carrying the 413.d retroviral integration were maintained on a 129/Sv background and genotyped by PCR as described (Conlon et al., 1994). Animals carrying the ROSA26 gene trap integration (Friedrich and Soriano, 1991) were obtained from the Jackson Laboratories (TgR(ROSA26)RSor strain, Jackson Laboratories, Bar Harbor). A similar gene trap line designated BT-5 (V. Episkopou and E.J.R., unpublished) was maintained on a 129×C57BL/6 hybrid background. The single independent copy of a *lacZ* reporter gene derived from the ROSA retroviral vector (Friedrich and Soriano, 1991) carried by both strains is ubiquitously expressed throughout embryogenesis (Friedrich and Soriano, 1991; V. Episkopou and E. J. R., unpublished). Heterozygous ROSA26 and BT-5 animals were identified by X-gal staining of ear tissue biopsies.

For analysis of *nodal.lacZ* expression during development, embryos were collected from matings between heterozygous *nodal*^{lacZ} males and 129/Sv or CD-1 (Charles River, Wilmington, MA) females and stained for β-galactosidase activity as described (Hogan et al., 1994), using either X-gal or Salmon-gal (Biosynth) as the substrate. Embryos were postfixed in 4% paraformaldehyde, embedded in paraffin wax and sectioned at 9 μm. Sections were dewaxed using standard procedures, mounted in either 80% glycerol or Permount and photographed under Normarski optics.

ES cell lines were isolated from blastocysts obtained from *413.d/+* females crossed to either *413.d/+*, ROSA26/+ or *413.d/+*, BT5/+ males, as described (Robertson, 1987). Individual ES cell lines were genotyped with respect to the *413.d* locus by Southern blot (Conlon et al., 1991). Genotyping for the ROSA26 or BT-5 allele was assessed by staining individual ES cell lines for β-galactosidase activity (Hogan et al., 1994). The experiments presented here were carried out using two independent *lacZ*$^{+}$ wild-type ES cell lines (R26.1 and BT5.7) and two *lacZ*$^{+}$ *413.d* homozygous *nodal*-deficient ES cell lines (ER.1 and ER.4).

Generation and analysis of chimeras

Chimeras were generated by blastocyst injection as described (Bradley, 1987). Blastocysts were collected from matings between *413.d* heterozygous animals, or from outbred CD-1 strain animals (Charles River, Wilmington, MA). For production of chimeric embryos with differing ES cell contributions, the number of ES cells injected into the blastocoel cavity was varied from 2-4 up to a maximum of 12-14 cells. Following transfer into pseudopregnant foster females, the manipulated embryos were recovered either at day 7.5 or 10.5 of development. Embryos were fixed and processed either for β-galactosidase staining or in situ hybridization. In experiments using embryos from *413.d* intercrosses, the genotype of the host blastocyst was determined retrospectively from a sample of extraembryonic tissue. Briefly, individual visceral yolk sacs were dissected from 10.5 day conceptuses, washed in PBS, and the endoderm layer isolated manually following digestion in pancreatic-trypsin as described (Hogan et al., 1994). DNA samples prepared from the endodermal fraction were genotyped with respect to the *413.d* locus by PCR as described (Conlon et al., 1994).

Whole-mount in situ hybridization and immunohistochemistry

Whole-mount in situ hybridization using digoxigenin-labelled RNA probes was performed as described (Wilkinson, 1992). Additionally, a fluorescein-labelled RNA probe detected with Magenta-Phos substrate (Biosynth) was used for double labelling as described (Levin et al., 1995). The *Shh En-1* and *Krox-20* probes have been described previously (Echelard et al., 1993; Davis and Joyner, 1988; Wilkinson et al., 1989). The *Wnt-8b* probe was kindly provided by Scott Lee and Andrew McMahon (S. Lee and A. McMahon, personal communication). Following photography, embryos were processed for sectioning.

RESULTS

nodal expression domains in early mouse embryos

nodal transcripts are present in ES cells (Conlon et al., 1994). Consistent with this, correctly targeted ES cell clones carrying the *nodal*^{lacZ} reporter allele stained uniformly for β-gal activity in the undifferentiated state (data not shown). To determine the onset of *nodal* expression in vivo, *nodal*^{lacZ} heterozygous embryos were examined for β-gal activity from 3.5 day post coitum (d.p.c.) onwards. No detectable activity was observed at the blastocyst stage (data not shown). However, shortly after implantation (5.5 d.p.c.) low levels of staining were detected throughout the embryonic ectoderm and associated overlying primitive endoderm (Fig. 1A). No *lacZ* expression was detected in the more proximally located extraembryonic ectoderm population (data not shown).

By approximately 6.0 d.p.c., just prior to overt streak formation, β-gal activity was detected in the embryonic epiblast and primitive endoderm (Fig. 1B). Low but uniform *lacZ* expression was seen throughout the visceral endoderm cell population (Fig. 1B-E) and was most noticeable in a morphologically distinct region of anterior endoderm lying approximately 10-15 μm distal to the junction of the embryonic and extraembryonic tissues, which retains a more thickened character. However, the more obvious staining seen in this population likely reflects increased cell density since analysis of numerous independent embryos revealed β-gal-positive cells in all regions of the visceral endoderm, including the proximal region overlying the extraembryonic ectoderm. By contrast, within the embryonic ectoderm nodal activity was highest in

the posterior proximal quadrant suggesting gene activity is downregulated on the prospective anterior side of the embryo. Interestingly expression remained radially symmetrical at levels coincident with or just distal to the region where the embryonic and extraembryonic cell populations abut (Fig. 1C). However, 10-15 μm distal to this region corresponding to the level at which a distinct thickening of the anterior visceral endoderm is visible, expression is clearly strongest on the prospective posterior side of the egg cylinder (Fig. 1D). Similarly towards the distal tip of the egg cylinder, *lacZ* expression was markedly higher on the posterior side (Fig. 1E). These results demonstrate that the primitive streak forms at the site of highest nodal activity within the ectoderm.

The pattern of *nodal* expression changes rapidly during the next few hours of development. By early streak stages, nodal activity was completely absent in the anterior ectoderm, although high levels persist on the posterior side of the embryo (Fig. 1F). Mesoderm cells exiting the streak proximally and laterally briefly retain *lacZ* expression (Fig. 1G,H). At this stage, we failed to detect *lacZ* expression in the overlying visceral endoderm. Within the ectoderm, *nodal* expression was rapidly lost as the streak elongates distally and, by late streak stages, only a few cells, strictly confined to the posterior side of the embryo, show weak β-gal staining (Collignon et al., 1996; data not shown). In sum, *nodal* is expressed prior to primitive streak formation. Expression continues during the initial stages of streak induction and is then rapidly down regulated as the streak elongates. Subsequently *nodal* expression is detected in a small subset of node progenitors, and following the formation of the morphologically distinct node becomes restricted to the edges of the notochordal plate (Collignon et al., 1996).

The block to gastrulation in *413.d nodal* mutant embryos is rescued by wild-type ES cells

Based on the results above, the gastrulation defect displayed by *nodal*-deficient embryos could potentially reflect an essential role for nodal signaling in the primitive endoderm, the embryonic ectoderm or both cell lineages. To distinguish these possibilities, we undertook a mosaic analysis using wild-type

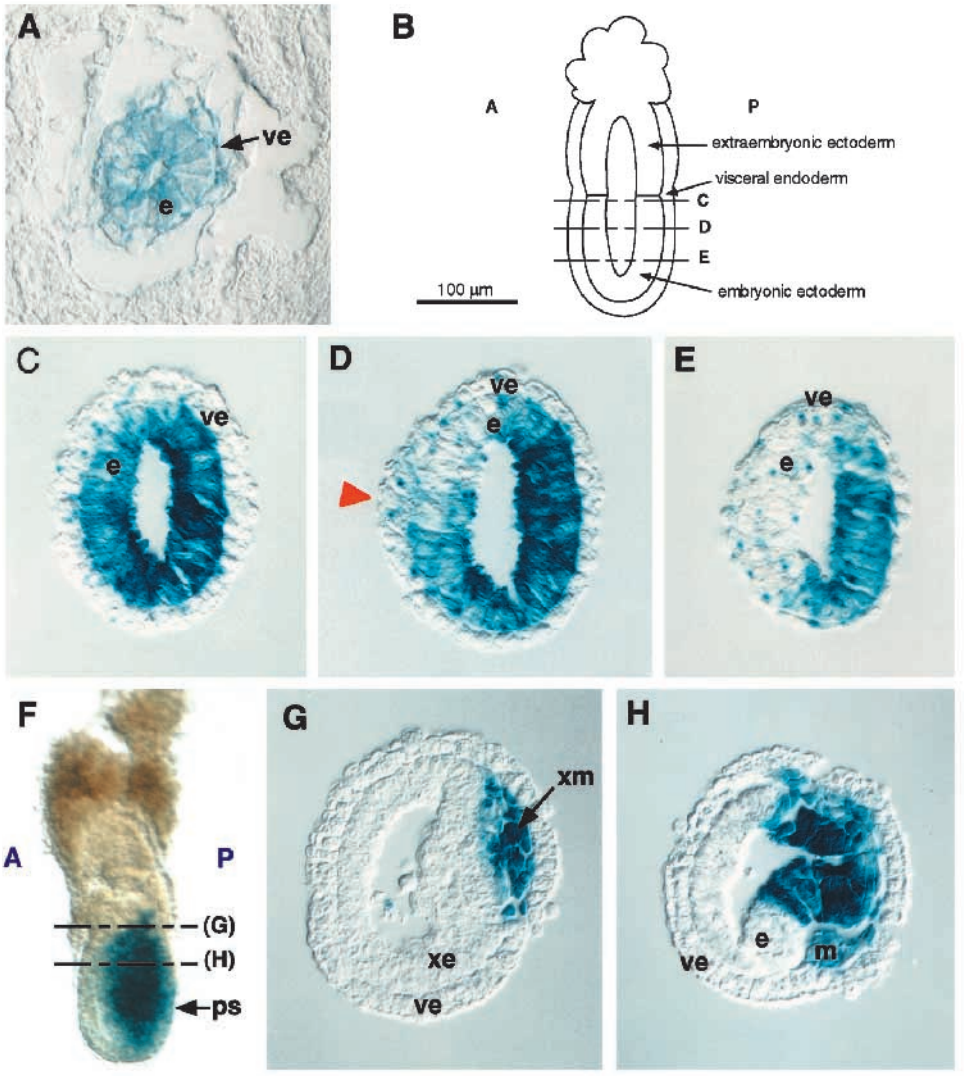

Fig. 1. Dynamic pattern of *nodal.lacZ* expression during gastrulation. Embryos heterozygous for the *nodal*^{lacZ} allele recovered at 5.5, 6.0 and 6.5 d.p.c. were stained with X-gal. (A) Transverse section through a 5.5 d.p.c. embryo within the deciduum. Low levels of expression are seen in both the visceral endoderm and the epiblast. (B) Schematic diagram of a 6.0 d.p.c. embryo (prior to streak formation) showing the appropriate locations of the transverse sections presented in C-E. Higher levels of nodal expression are broadly distributed in the epiblast adjacent to the extraembryonic junction (C). In more distal regions, *lacZ* becomes localized to the presumptive posterior side of the embryo (D,E). Low levels of expression are seen throughout the visceral endoderm (C-E) and in the anterior epiblast (D,E). A distinct patch of thickened visceral endoderm (red arrowhead) can be seen at the prospective anterior side of the embryo in the section shown in D. (F) *nodal* expression at early streak stages. *lacZ* expression is confined to the posterior side of the 6.5 d.p.c. embryo. The plane of the transverse sections shown in G and H are indicated. The section in G corresponds to a level slightly above the extraembryonic junction and shows extraembryonic mesoderm migrating from the streak and β-gal staining confined to the most proximal embryonic ectoderm. In the embryonic region (H), *nodal* expression is maintained at a high level in the ectoderm adjacent to the streak but declines in the nascent mesoderm emerging from the streak. At this stage, *nodal* expression is not detected in the anterior ectoderm or in the visceral endoderm. The anterior side of the embryo is towards the left in C-H. Abbreviations: e, embryonic ectoderm; m, embryonic mesoderm; ps, primitive streak; ve, visceral endoderm; xe, extraembryonic ectoderm; xm, extraembryonic mesoderm; A, anterior side; P, posterior side of the embryo.

and *nodal*-deficient ES cells. It is known that ES cells display a marked developmental bias when introduced into recipient blastocysts, almost exclusively colonizing the embryonic epiblast (Beddington and Robertson, 1989). Thus mosaic embryos contain ES cell derivatives largely confined to the embryonic portion, while the primitive endoderm and its derivatives are of host origin. In the present experiments, we used ES cell lines carrying ubiquitously expressed *lacZ* transgenes (Friedrich and Soriano, 1991) to simultaneously mark and follow the fates of the injected ES cells. It was first important to confirm that ES cell derivatives preferentially colonise the epiblast lineage in chimeras obtained from blastocyst injection. A panel of chimeric embryos (n=12), obtained by injecting wild-type *lacZ*-marked ES cells, were retrieved at early gastrulation stages, stained for β-gal activity and serially sectioned. As shown in Fig. 2, we found no evidence for the presence of *lacZ*-expressing cells in either the extraembryonic ectoderm or primitive endoderm lineage in embryos in which the epiblast was strongly colonised by ES cell derivatives.

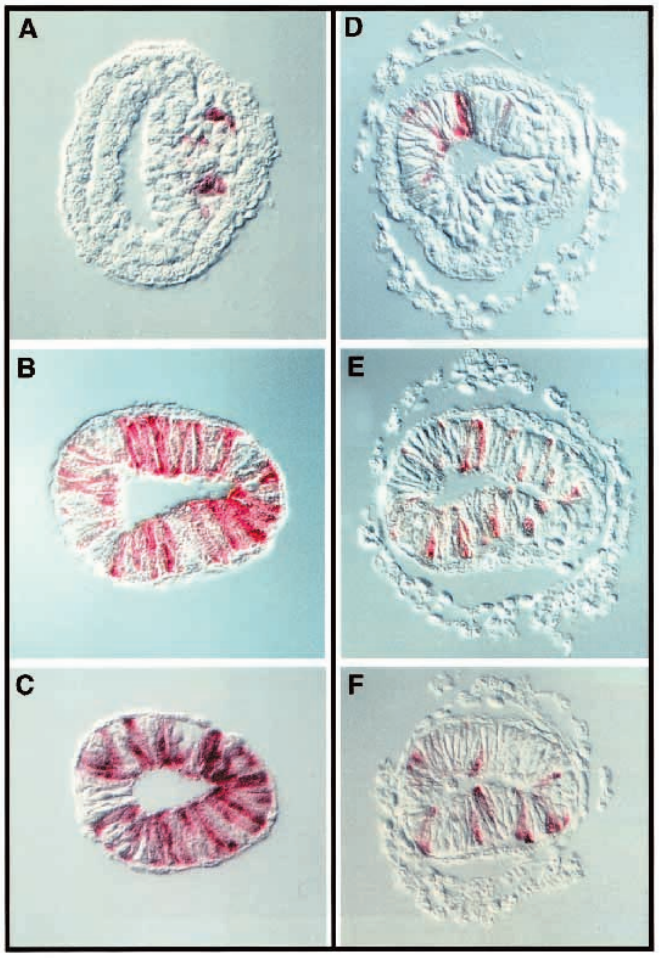

Fig. 2. ES cell derivatives fail to colonize the extraembryonic and primitive endoderm lineages in chimeric embryos. Chimeric embryos generated by injecting wild-type *lacZ*-expressing ES cells into wild-type embryos were recovered at early gastrulation stages, stained in Salmon-gal and serially sectioned. (A-C, D-F) Three transverse sections from two independent embryos, respectively. (A,D) Sections correspond to a level slightly above the extraembryonic junction, (B,E) sections correspond to a region midway down the embryonic regions and (C,F) sections correspond to regions close to the distal tip of the egg cylinder. *lacZ*-expressing cells are confined to the embryonic ectoderm and nascent mesoderm. The anterior side of the embryos is to the left.

To test the role of nodal activity in the primitive endoderm and epiblast, we used the strategy outlined schematically in Fig. 3. Thus wild-type ES cells were injected into *413.d* mutant blastocysts to generate chimeric conceptuses in which the primitive endoderm was composed exclusively of *nodal*-deficient cells (class I chimeras). Alternatively, in the reciprocal experiment, *nodal*-deficient ES cells injected into wild-type blastocysts gave chimeras in which the primitive endoderm was genetically wild type (class II chimeras). In control experiments, wild-type ES cells were injected into wild-type blastocysts (class III chimeras).

We initially tested whether the introduction of wild-type ES cells could rescue the gastrulation defect in *413.d* mutant embryos. Increasing numbers of wild-type *lacZ*$^+$ ES cells were injected into host blastocysts recovered from intercross matings between *413.d* heterozygous animals. Chimeras were identified by β-gal staining of 10.5 d.p.c. conceptuses (Table 1). All of these were judged to have undergone gastrulation, since they were developing within a distinctive visceral yolk sac (VYS). Approximately 15% of the chimeras (21/138) proved to be derived from *413.d* mutant blastocysts (class I chimeras). These embryos had clearly gastrulated to produce extraembryonic mesodermal tissue, but were all morphologically abnormal and smaller in comparison to their littermates (Fig. 4). The extent of development of the A-P axis in these

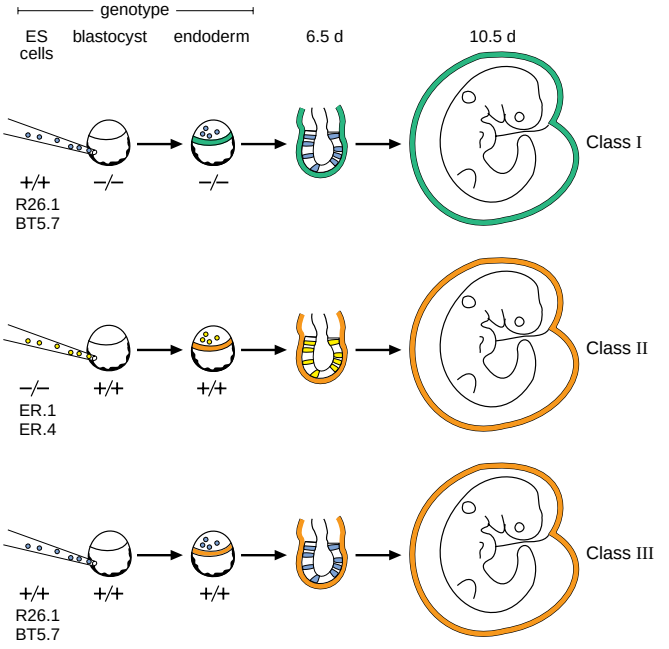

Fig. 3. Experimental strategy for evaluating nodal activities in the ectoderm and primitive endoderm cell lineages. Injection of *lacZ*$^+$ wild-type ES cells (blue) into *413.d nodal*-deficient blastocysts leads to the generation of mosaic embryos in which the primitive endoderm (green) is exclusively *nodal*-deficient in origin (class I chimeras). Alternatively, injection of *lacZ*$^+$ *nodal*-deficient ES cells (yellow) into wild-type blastocysts results in mosaic embryos in which the primitive endoderm (orange) is wild type (class II chimeras). As a control, wild-type ES cells were injected into wild-type blastocysts (class III).

Table 1. (A) Genotypes and extent of colonization by *lacZ*-marked ES cell derivatives in chimeric embryos recovered at 10.5 days of development

No. embryos recovered	No. chimeras*	% contribution of ES cells†	Genotype of injected blastocyst‡ +/+	d/+	d/d (class I)
152	138				
		>30%	18	28	12
		10-30%	13	16	5
		<10%	14	28	4
		TOTAL	45	72	21
			(32.6%)	(52.2%)	(15.2%)

(B) Extent of A-P axis development in class I chimeras scored at day 10.5 p.c.

No. embryos scored	Extent of colonization by wild-type cells	No. embryos showing overt morphological features: Neural folds	Somites	Heart tube	Otic vesicle	Branchial arches	Optic vesicle
12	>30%	12	12	12	12	0	0
5	10-30%	5	3	5	4	0	0
4	<10%	2	0	0	0	0	0

*Chimeras were identified by X-gal staining.

†Percentage chimerism was estimated from whole-mount inspection of individual stained embryos. Random embryos were embedded and sectioned to ensure that the degree of overt chimerism reflected the actual percentage of β-gal-positive cells. The variation in the extent of colonization was achieved by injecting variable numbers (between 2 and 14) of ES cells.

‡The genotype of the originally injected blastocyst was determined retrospectively by PCR analysis of DNA prepared from the endoderm fraction of the VYS.

rescued animals correlated strongly with the degree of colonization by wild-type *lacZ*$^+$ ES cells (Table 1B). When the wild-type contribution was 10% or less, the chimeric embryos resembled simple cylinders of cells lacking overt morphological hallmarks (Fig. 4A). A rudimentary allantois had formed in these embryos. This, together with the point of insertion of the VYS, allowed the identification of the posterior end of the axis. Derivatives of the *lacZ*$^+$ wild-type ES cells were scattered randomly along the extent of the rudimentary axis (Fig. 4A), reflecting substantial mixing with host epiblast cells prior to gastrulation (Lawson et al., 1991; Lawson and Pedersen, 1992).

More strongly colonized embryos (10-30% wild-type contribution) displayed a more robust A-P axis (Fig. 4B), with morphologically distinct anterior and posterior structures. A well-developed neural tube was frequently visible in this class of chimera, although it was often kinked in appearance. Distinctive somites, derivatives of paraxial mesoderm, were occasionally observed, but were abnormally shaped and fused across the midline (Fig. 4B). By contrast, extensively colonized chimeras (wild-type contribution 30% or higher) were relatively well developed. These frequently possessed a grossly normal heart (Fig. 4C,E), which in all cases was visibly beating at the time of dissection. Additionally, as shown in Fig. 4E, an orderly array of paired somites was visible in more posterior regions of the axis and some of these embryos had undergone turning. In the majority of extensive chimeras, the trunk and caudalmost structures appeared grossly normal (Fig. 4C,E). However, we observed pronounced abnormalities affecting the development of anterior neural structures. For example, as shown in Fig. 4C,E, the neural structures rostral to the otic vesicle are clearly defective. In the example shown in Fig. 4E, the region of the forebrain and midbrain appears to be largely missing and a single, narrow, fused head structure is present anterior to the otic vesicle.

Defects in the formation of the anterior neural axis have been described in embryos carrying loss-of-function mutations in the *HNF-3β* (Ang and Rossant, 1994; Weinstein et al., 1994), *Lim-1* (Shawlot and Behringer, 1995) and *Otx-2* (Acampora et al., 1995; Matsuo et al., 1995; Ang et al., 1996) genes. These three genes are expressed in both the visceral endoderm and in derivatives of the embryonic ectoderm (Monaghan et al., 1993; Acampora et al., 1995; I. V., J. C. and E. J. R., unpublished data). Strikingly, all three mutations result in a similar phenotype during gastrulation. Thus, homozygous mutant embryos exhibit a characteristic narrowing or constriction at the junction of the extraembryonic and embryonic ectoderm at early to mid-streak stages. In all cases, this defect is associated with a greatly reduced primitive streak and impairment of the normal cell movements associated with gastrulation.

We wanted to know if the anterior defects described above in class I chimeras were also associated with similar morphological abnormalities during gastrulation. To test this, blastocysts from *413.d/+* heterozygous intercrosses were injected with wild-type *lacZ*$^+$ ES cells and the resulting chimeric embryos examined at 7.5 days of gestation. As shown in Fig. 5, approximately 25% of chimeras (3/13 analyzed) were aberrantly shaped and showed a pronounced constriction at the embryonic-extraembryonic region, even in cases where the embryonic ectoderm was extensively colonized by *lacZ*$^+$ cells and thus largely wild type in character (Fig. 5C,D). Only a quarter of the embryos exhibited this abnormality suggesting they probably correspond to chimeras derived from *413.d* homozygous mutant blastocysts.

Molecular characterization of the anterior defects in chimeras

To more clearly delineate the nature of the anterior truncations described above, day 10.5 chimeras were further analyzed by assessing the expression of *Krox-20*, *En-1* and *Wnt-8b* mRNAs,

specific markers of hindbrain, midbrain and forebrain tissue subpopulations, respectively (Table 2). At 9.5 days of development, *Krox-20* is known to be expressed in rhombomeres 3 and 5 and by day 10 is confined to rhombomere 5 (Wilkinson et al., 1989). *Wnt-8b* marks the dorsal region of the telencephalon and expression extends rostrally into the diencephalon at 10.5 days of development (S. Lee and A. McMahon, personal communication). In double labeling in situ hybridization experiments control chimeric embryos (class III) showed the expected patterns of *Krox-20* and *Wnt-8b* expression (Fig. 6A). In contrast, extensively rescued chimeras generated from *nodal* mutant blastocysts express *Krox-20* in the region of the otic vesicle, but there was no evidence for the expression of *Wnt-8b* (Fig. 6A,B). To further characterise the anterior neural tissue populations, additional chimeras were analysed for the expression of *En-1*. At 10.5 d.p.c., *En-1* is strongly expressed throughout a ring of neural tissue at the hindbrain-midbrain junction (Davis and Joyner, 1988; Fig. 6C). In keeping with the *Krox-20* results, none of the poorly rescued chimeras analysed showed evidence for expression of *En-1* mRNA in the developing CNS, although a specific hybridization signal was present in the developing somites and limb buds. However, in two extensively rescued chimeras, the hindbrain-midbrain region, or isthmus, had clearly been induced as evidenced by the presence of a characteristic stripe of *En-1* expression (Fig. 6D,E). Collectively these gene marker studies show that, while posterior regions of the midbrain encompassing the hindbrain-midbrain boundary do form, the rostral-most neural structures fail to form in this class of chimeras. In particular, we note that none of the strongly rescued chimeras show evidence for the formation of forebrain tissue.

The anterior truncations seen in mutant embryos lacking either *Lim-1* or *Otx-2* (Shawlot and Behringer, 1995; Acampora et al., 1995; Matsuo et al., 1995; Ang et al., 1996) suggest these molecules are essential for specification of the prechordal plate, node and notochord during gastrulation. These axial mesoderm populations derived from the anterior streak are known to participate in the rostrocaudal patterning of the CNS (reviewed Shimamura et al., 1995; Placzek et al., 1993). To assess whether similar defects in ventral midline structures contribute to the anterior axis abnormalities described above, chimeras derived from *nodal* mutant blastocysts were examined for expression of *Shh* mRNA. At 10.5 d.p.c., *Shh* mRNA is normally present in the notochord and ventral floor plate along the length of the spinal cord and hindbrain. In the mid and forebrain regions, expression expands to occupy more dorsal regions and extends anteriorly to the rostralmost region of prosencephalon (Echelard et al., 1993; Shimamura et al., 1995). All five of the class I chimeras analyzed at 10.5 d.p.c. expressed *Shh* mRNA in midline structures including the notochord, floor plate and gut structures (Fig. 7A-E). However, we observed intermittent expression caudal to the hindbrain region (recognized by the presence of the otic vesicle), suggesting these embryos fail to form a continuous notochord. Considering the node gives rise to the notochord (Beddington, 1994; Sulik et al., 1994), these defects probably reflect functional abnormalities of the node at early stages of development. Sections through the most anterior regions of these chimeras (Fig. 7D) showed no discernable notochord. *Shh*-expressing cells were confined to a narrow stripe of ventrally placed neuroectodermal cells, a pattern similar to that seen in the normal hindbrain-midbrain region of wild-type embryos (Shimamura et al., 1995). Together these marker gene studies, summarised in Table 2, demonstrate that the forebrain and possibly anterior portions of the midbrain

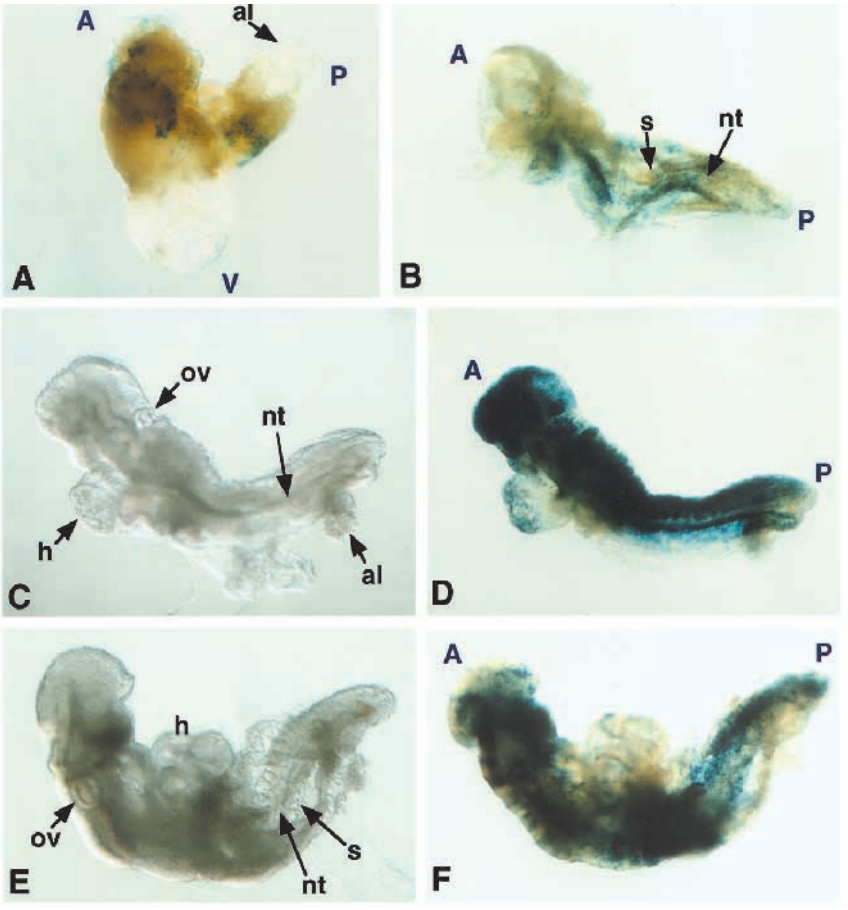

Fig. 4. Wild-type ES cells can rescue the block to gastrulation in *nodal*-deficient embryos. *413.d* mutant blastocysts were injected with variable numbers of ES cells, allowed to develop to 10.5 d.p.c. and stained in X-gal to assess the distribution of *lacZ*$^+$ wild-type ES cells. (A) A chimera where the wild-type *lacZ*$^+$ ES cell contribution is less than 10%. This embryo has gastrulated to form a simple cylinder structure. The orientation of the A-P axis is indicated by the presence of a rudimentary allantois at the posterior end. (B) A chimera showing increased (approx. 15-20%) wild-type *lacZ*$^+$ ES cell contribution. This embryo has formed abnormal somites that are fused across the midline. (C-F) Two chimeras with an approximately 30% wild-type contribution, before (C,E) and after (D,F) processing for X-gal staining, respectively. Largely normal trunk and posterior regions can be seen, however the anterior regions are truncated. Abbreviations: a, allantois; h, heart; nt, neural tube; ov, otic vesicle; s, somites.

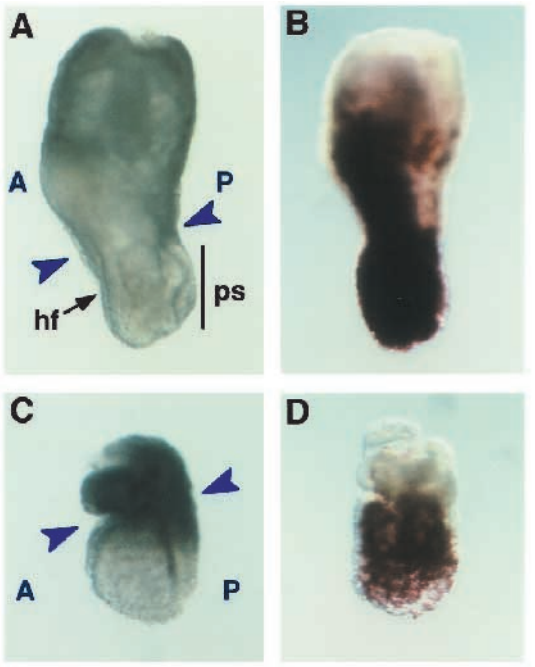

Fig. 5. Abnormal gastrulation generated from *413.d* mutant blastocysts (class I chimeras). (A,C) Two examples of 7.5 d.p.c. chimeras exhibiting a constriction (blue arrowheads) at the embryonic/extraembryonic boundary. (B,D) Same embryos as in A and C, stained with salmon-gal to show the distribution of wild-type *lacZ*$^+$ ES cell derivatives. Abbreviations: hf, headfold; ps, primitive streak.

structures fail to form in chimeric conceptuses derived from homozygous *413.d* blastocysts.

A requirement for nodal signaling in the primitive endoderm

Results above clearly indicate that *nodal*-deficient endoderm can support gastrulation, showing that nodal signaling in the primitive endoderm is not required for primitive streak formation within the epiblast. However, even when wild-type cells extensively colonize the founder epiblast population, we observe incomplete formation of the most rostral aspects of the neural axis. The prechordal plate is responsible for induction of the midbrain and forebrain (Placzek et al., 1993). However, the morphogenesis and progenitor cell populations of this tissue remain poorly defined (Sulik et al., 1994). Thus either the lack of nodal signaling in the primitive endoderm lineage, or reduced nodal signaling in the embryonic ectoderm during early gastrulation could potentially disturb the formation of anterior midline populations.

To distinguish these possibilities, we first examined whether formation of the prechordal plate was affected in chimeras extensively colonized by *nodal*-deficient ES cells. We compared the development and colonization patterns of *nodal*-deficient and wild-type ES cells injected into wild-type blastocysts (class II and class III chimeras, respectively; Fig. 3). Chimeric embryos analyzed at early headfold stages (7.5 d.p.c.) were found to be grossly morphologically normal irrespective of the genotype of the injected ES cells. To examine the possibility that *nodal* mutant cells might be selectively excluded from specific cell populations such as the prechordal

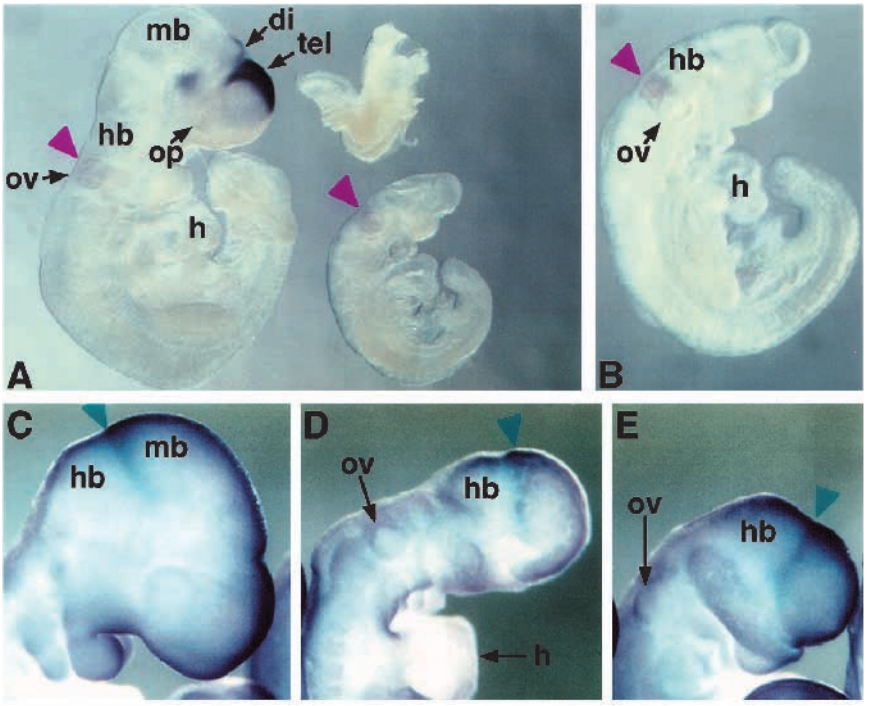

Fig. 6. Anterior neural defects found in class I chimeras at 10.5 d.p.c. (A) Whole-mount in situ hybridization analysis of *Wnt-8b* (purple stain) and *Krox-20* (light pink stain, arrowhead) expression in wild type (left) and two class I chimeras (right). *Wnt-8b* expression is absent in both rescued chimeras. *Krox-20* expression in r5 is detected in the chimera exhibiting the most extensive rescue (shown at higher magnification in B). (C-E) Whole-mount in situ hybridization analysis of *En-1* expression in wild type (C) and two extensively rescued class I chimeras (D,E) at day 10.5 p.c. (C) High magnification view of the anterior region of a wild-type embryo. The *En-1* expression domain includes the isthmus, with expression extending both anteriorly and posteriorly into the midbrain and hindbrain, respectively. A pronounced D-V band of hybridization demarcates the hindbrain-midbrain boundary. (D,E) High magnification view of two chimeras showing expression of *En-1* ; the hindbrain-midbrain region has clearly formed in both embryos (arrowheads) in a region of the developing brain rostral to the otic vesicle. The more posterior regions of the trunk were well developed in both embryos and closely resembled the chimera shown in B. Note that the apparent signal in the forebrain region of the control embryo is due to background: in this experiment, the embryos were incubated in substrate for a longer period of time to maximize the staining in the chimeric embryos. Three additional less well rescued chimeras showed no evidence for staining in the anterior regions, although the somites and limb buds showed the predicted pattern of *En-1* expression (data not shown).

Table 2. Analysis of rostral CNS development in class I chimeras assessed by expression of region-specific markers

Probe	No. chimeras hybridized*	No. showing CNS expression†
Shh	5	5
Krox-20	4	2
En-1‡	13	2
Wnt-8b	4	0

*As a positive control for the hybridization conditions, chimeric embryos were processed together with wild-type embryos.

†For the *Krox-20* and *En-1* probes, a positive hybridization signal was only seen in those chimeras showing extensive rescue of the normal body axis.

‡To ensure that low levels of *En-1* expression were detected, embryos were incubated in substrate for longer than optimal time periods. A low level of background staining in the surface ectoderm was present in both the control and chimeric embryos.

plate or midline, chimeras were serially sectioned. As shown in Fig. 8, *nodal*-deficient cells exhibit a perfectly normal colonization pattern. Thus derivatives of *nodal* mutant ES cells extensively contributed to dorsal and ventral regions of the node, and anterior mesoderm populations (Fig. 8D,E, data not shown). As expected (Beddington and Robertson, 1989; see Fig. 2), ES cell derivatives fail to colonize the primitive endoderm lineage. Thus *lacZ*$^+$ cells were not detected in the visceral yolk sac endoderm population. Interestingly, in sections of headfold-stage chimeras, numerous β-gal ES cell derivatives were seen in the outermost layer of cells overlying the mesoderm in the embryonic region (Fig. 8D,E). β-gal staining thus identifies derivatives of the midline that contribute to the definitive endoderm population. These data confirm previous studies indicating that the definitive embryonic endoderm rapidly displaces the primitive endoderm during gastrulation (Lawson and Pedersen, 1987; Tam and Beddington, 1992; Thomas and Beddington, 1996). Additionally, we noted several highly chimeric embryos that displayed a marked absence of *lacZ*-expressing cells in the notochordal plate and midline (Fig. 8A,B). Conversely, in weakly colonized chimeric embryos, ES cell derivatives were occasionally confined to the midline (Fig. 8C). Together these observations suggest that a small number of founder epiblast cells contribute to the formation of the node and its derivatives and that little cellular mixing occurs following allocation of this population.

Interestingly, none of the large number (*n*=30) of class II chimeras examined at mid streak to early head fold stages, in which the majority of the epiblast derivatives were *nodal*-deficient, showed overt abnormalities. Thus, the pronounced morphological constriction seen at gastrulation in class I chimeric embryos resulting from the injection of *413.d nodal*-deficient blastocysts (Fig. 5), can be specifically attributed to the absence of *nodal* expression in the primitive endoderm lineage. Finally, to exclude the possibility that chimeras containing a large component of *nodal* mutant cells develop anterior patterning defects at later stages, the embryonic development of class I and class II chimeras was compared at 10.5 d.p.c. Clear anterior defects were present in extensively chimeric embryos obtained from *nodal* mutant blastocysts (Fig. 9C-F). In marked contrast, all of the class II chimeras examined (*n*=20) in which *lacZ*$^+$ *nodal*-deficient ES cell derivatives constituted greater than 80% of the embryo showed correct patterning of the anterior CNS structures (Fig. 9A,B). In both classes of chimera, the *lacZ*-marked wild-type and *nodal*-deficient cells respectively were uniformly distributed along the entire extent of the A-P and dorsal-ventral axis. Collectively these experiments show that the anterior defects documented in chimeras generated from *nodal* mutant blastocysts results from loss of nodal signaling in the primitive endoderm during early gastrulation.

DISCUSSION

Elegant single cell marking studies in the mouse have shown that the cells of the early epiblast are regionalized with respect to their fate prior to the initiation of gastrulation (Lawson et al., 1991; Lawson and Pedersen, 1992). However, relatively little is known about the molecular signaling pathways that

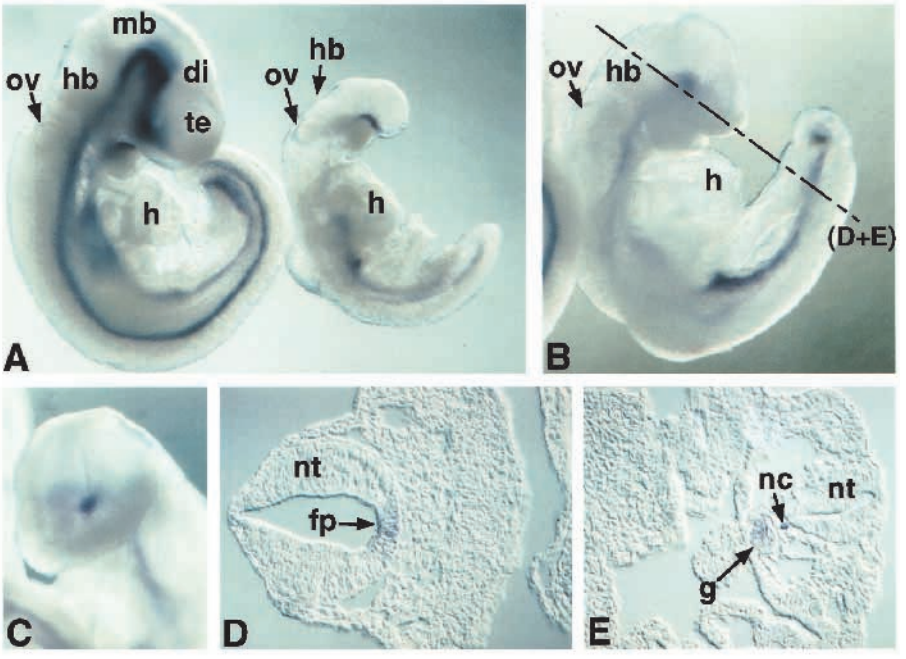

Fig. 7. Expression of *Shh* mRNA in mid-gestation embryos. (A) *Shh* expression in wild type (left) and class I chimeras (right) at 10.5 days. (B,C) Lateral and frontal views, respectively, of a second class I chimera. In addition to the obvious defect in the anterior expression pattern, both chimeras show discontinuous staining of the notochord and/or gut. (A,B) Transverse sections of the chimera in B and C taken at anterior and posterior levels, respectively, to show *Shh* expression in the ventral part of the neural tube (D) and in notochord and gut posteriorly (E). Abbreviations: di, diencephalon; fp, floorplate; g, gut; hb, hindbrain; h, heart; mb, midbrain; nt, neural tube; op, optic vesicle; ov, otic vesicle; nc, notochord; te, telencephalon.

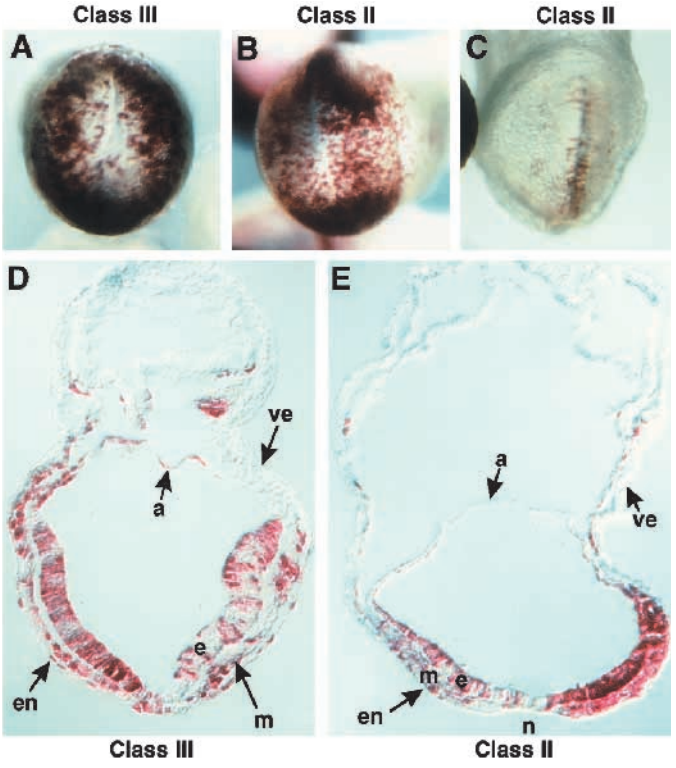

Fig. 8. Distribution of wild-type (class III chimeras) and *nodal*-deficient (class II chimeras) ES cell derivatives, following injection of wild-type blastocysts. Early headfold-stage (7.5 d.p.c.) embryos are stained for *lacZ* expression. (A,B) Ventral views and the corresponding frontal sections are shown in D and E, respectively. Wild-type (A) and *nodal* (B)-deficient ES cells colonize all embryonic germ layers, ectoderm, mesoderm and endoderm. β-gal-stained cells are absent from the visceral endoderm of the VYS. Both embryos exhibit a conspicuous exclusion of ES derivatives at the midline. In contrast the chimera shown in C shows descendants of *nodal*-deficient ES cells occupying the midline structures. Abbreviations: a, amnion; e, ectoderm; en, definitive endoderm; m, mesoderm; ve, visceral endoderm.

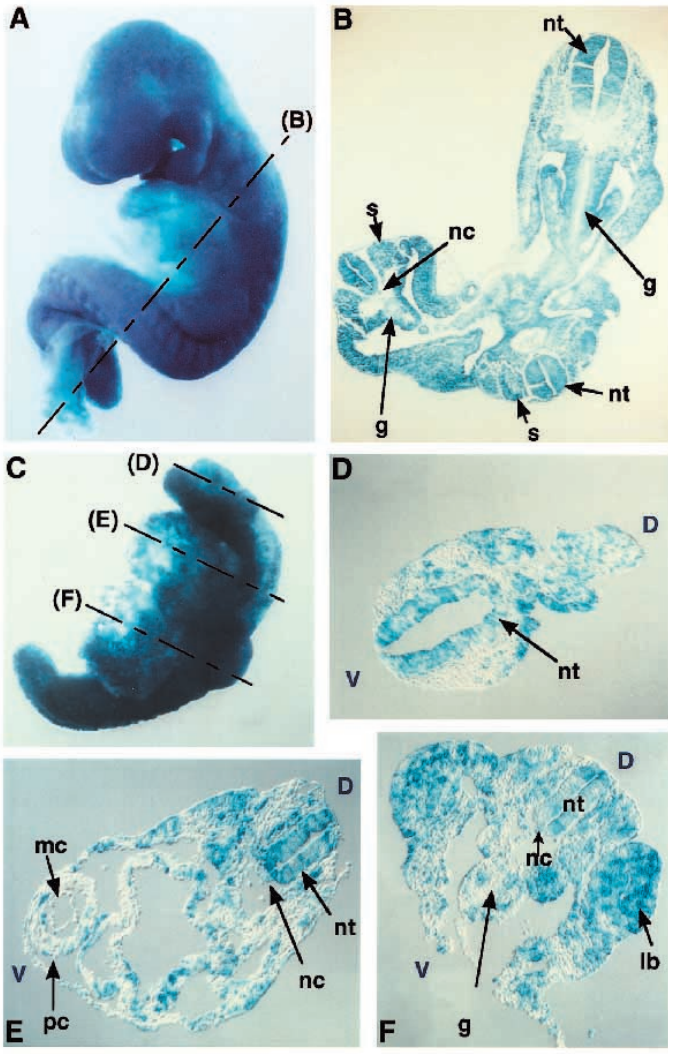

Fig. 9. Chimeras in which the primitive endoderm is *nodal*-deficient exhibit anterior defects at 10.5 days. Class II chimera (A) in comparison with class I chimera (C). In the class II chimera, *lacZ*$^+$ *nodal*-deficient ES cell derivatives are distributed uniformly along the A-P and D-V axes (B). (C) A class I chimera composed of >50% wild-type *lacZ*$^+$ cells displays severe anterior abnormalities. Histological sections at anterior (D), future thoracic (E) and more posterior regions (F) of this chimera show extensive colonization by wild-type ES cell derivatives and the absence of anterior structures. Abbreviations: ht, heart; g, gut; lb, limbud; nc, notochord; nt, neural tube; V, ventral side; D, dorsal side of the embryo.

position the primitive streak within the radially symmetrical epiblast or the activities required to initiate the process of streak formation. A number of genes initially expressed uniformly in the epiblast become asymmetrically localized prior to overt streak formation. For example, both *Fgf-8* (Crossley and Martin, 1995) and *nodal* appear to be expressed in a gradient, with highest levels of activity confined to the prospective caudal region of the future axis. Thus a strong argument can be made that the epiblast acquires molecular asymmetry prior to overt streak induction.

The finding that *nodal*-deficient embryos fail to gastrulate (Conlon et al., 1994) has been taken as evidence that, as for other TGFβ members acting in lower vertebrates, nodal normally induces the formation of nascent mesoderm (Conlon and Beddington, 1995). However, there is also evidence that both mouse nodal and Xnr-3 may regulate the migratory properties of cells (Conlon et al., 1994; Smith et al., 1995). Consistent with this, the present analysis of *nodal.lacZ* expression indicates that *nodal* is only transiently detected during early streak formation. Thus its activity is not required continuously during gastrulation as might be expected if it acts primarily as a mesoderm-inducing activity, or is required to maintain the structure of the streak region.

The present chimera experiments indicate that very low levels of nodal activity provided by a minor population of wild-type cells are sufficient to alleviate the block to gastrulation in *nodal*-deficient epiblast tissue. This is illustrated in Fig. 4, where the introduction of a small number of *lacZ*$^+$ wild-type ES cells is sufficient to allow a *nodal* mutant embryo to develop a well-elaborated A-P axis. However, we also note that the introduction of small numbers of wild-type ES cells into mutant blastocysts does not always rescue gas-

trulation. In our experiments analyzing a large panel of chimeric embryos (n=138) at 10.5 d.p.c. only 15%, as opposed to the expected 25%, were derived from *nodal* mutant blastocysts. The inability to rescue a proportion of mutant embryos likely stems from failure of *nodal*-expressing wild-type cells to occupy the prospective caudal region of the epiblast. These results suggest that localized nodal signaling within the embryonic ectoderm is necessary to promote the formation of the primitive streak.

At 10.5 days of development, many of the partially rescued chimeras resemble *HNF-3β* mutants. *HNF-3β* mutant mice fail to form a node or notochord, although they gastrulate to form a well-patterned A-P axis (Ang and Rossant, 1994; Weinstein et al., 1994). Numerous weakly colonized class I chimeras exhibit a similar phenotype suggesting that node morphogenesis is highly abnormal. Since these embryos are largely composed of *nodal*-deficient cells, the probability that significant numbers of wild-type cells become incorporated into the node progenitor population is very low. Thus it seems likely that *nodal* expression in the cells at the distal tip of the streak is normally required for node morphogenesis. Additionally, strongly colonized embryos analyzed at 10.5 d.p.c., exhibit discrete gaps in the A-P *Shh* expression domain. Thus the orderly production of the notochord is disturbed. It seems likely that *nodal* expression in the ventral lateral edges of the mature notochordal plate is important in maintaining the integrity of this structure and the orderly generation of the notochord and midline derivatives. Interestingly, the *nodal.lacZ* domain in the distal region of the streak is induced at the most caudal limit of the Shh expression domain. Thus *nodal* expression may be activated by short-range, possibly contact-mediated, Shh signaling. Consistent with this suggestion, ectopically supplied Shh protein has been shown to induce the expression of the nodal homolog *Cnr-1* in manipulated chick embryos (Levin et al., 1995). It will be interesting to learn whether *nodal* expression is disturbed in *Shh* mutant embryos.

Shortly after implantation *nodal* is transiently expressed in the layer of primitive endoderm cells that invests the epiblast tissue. Cell marking and mosaic experiments have shown that the primitive endoderm lineage contributes exclusively to the extraembryonic tissues (reviewed Tam and Beddington, 1992). Beyond possible roles in supporting the growth of the underlying ectoderm, the primary function of the visceral endoderm remains poorly understood. Because *nodal* is expressed in both the endoderm and ectoderm lineages, we devised an experimental strategy that allowed us to test whether *nodal* expression was essential for any aspects of endoderm function. These studies show that the transient expression of *nodal* in the visceral endoderm is not required for the initiation of gastrulation.

Strikingly nodal signaling in this cell layer appears essential to confer correct anterior patterning of the neural plate at later stages of development. Thus mosaic embryos comprised largely of wild-type cells developing in combination with mutant primitive endoderm lack the most rostral aspects of the axis. Conversely, mosaic embryos composed largely of *nodal* mutant ectoderm derivatives developing in conjunction with wild-type primitive endoderm form a normal A-P axis. We found that the forebrain, and possibly anterior midbrain, structures fail to form in the absence of *nodal*-expressing primitive endoderm. As induction of the forebrain, and possibly regions of the midbrain, in the vertebrate CNS is contingent on signals provided by the prechordal plate tissue (reviewed Shimamura et al., 1995), it seems likely that formation of this tissue is adversely affected in these chimeras. A number of morphological studies have shown that the prechordal plate forming at the rostral midline of the embryo is composed of a complex population of closely associated endoderm and anterior mesoderm cells (Poelmann, 1981; Sulik et al., 1994). While the embryonic origins of the endoderm cells that contribute to the prechordal plate have yet to be established, our experiments demonstrate that *nodal* expression in the primitive visceral endoderm prior to gastrulation is required for the correct morphogenesis of this population of cells, and hence the establishment of correct anterior positional identity in the developing neural tissue.

Recently evidence has been provided for important inductive interactions between the primitive endoderm and underlying ectoderm during early embryogenesis. Thus expression of the homeobox gene *Hesx1/Rpx* (Thomas and Beddington, 1996), first detected at the start of gastrulation, is confined to a small anterior domain of primitive endoderm, but a few hours later becomes apparent in the underlying anterior ectoderm. This second domain of ectodermal *Hesx1* expression is in part dependent on signals from the endoderm, since expression in the ectoderm is lost or severely depleted by physical removal of the anterior endoderm at earlier stages (Thomas and Beddington, 1996). A similar finding has been reported for *Otx-2*. Thus a *lacZ* reporter allele of *Otx-2* is initially activated in the visceral endoderm layer of *Otx-2* mutant embryos, but then fails to be expressed in the underlying anterior ectoderm (Acampora et al., 1995), suggesting that expression of *Otx-2* itself in the anterior endoderm is normally required for its subsequent induction in the ectoderm. Moreover, loss of *Lim-1*, normally expressed at early head fold stages in anterior mesoderm (Barnes et al., 1994; Shawlot and Behringer, 1995) and also in the anterior visceral endoderm (I. V., J. C. and E. J. R., unpublished data) results in a loss of the anterior neuroectodermal *Otx-2* expression domain (Shawlot and Behringer, 1995). In keeping with these findings, a series of elegant tissue recombination experiments have endorsed an important role for anterior mesendoderm populations in patterning the developing neural plate (Ang and Rossant, 1993; Ang et al., 1994).

Mosaic embryos developing within a *nodal*-deficient visceral endoderm exhibit a distinctive physical constriction between the embryonic and extraembryonic regions, similar to that seen in *HNF-3β*-, *Otx-2*- and *Lim-1*-deficient mutants. Since these mutants also exhibit defects in the formation of anterior regions of the neural axis, it is tempting to speculate that these molecules participate in a common pathway that is initiated prior to gastrulation by signals provided from the primitive endoderm. Evidence is now accumulating that the primitive endoderm is patterned with respect to the prospective A-P axis at early stages of postimplantation mouse development. Thus, at gastrulation, expression of *Hesx1/Rpx* (Hermesz et al., 1996; Thomas and Beddington, 1996), and the antigenic epitope VE-1 (Rosenquist and Martin, 1995) is localized to a distinct patch of prospective anterior visceral endoderm lying slightly distal to the junction with the extraembryonic ectoderm. This molecular and physical asymmetry may reflect

a role for the visceral endoderm in establishing anterior identity within the cells of the underlying ectoderm (Thomas and Beddington, 1996). It will be interesting to examine whether *nodal*, expressed throughout the visceral endoderm of the pregastrulation-stage embryo, participates in setting up this marked regional identity within the endoderm. Most recently a novel secreted molecule, cerberus, normally expressed in the anterior endoderm of Spemann's organizer has been shown to induce ectopic head structures in manipulated *Xenopus* embryos (Bouwmeester et al., 1996). Collectively these findings, in conjunction with the experiments in mouse discussed above, serve to underscore an important involvement of the anterior endoderm in the induction of anterior regions of the vertebrate body axis.

We thank Liz Bikoff for valuable comments on the manuscript, Vasso Episkopou for kindly providing the BT-5 gene trap mice and Rosa Beddington for insightful discussions. We thank Scott Lee and Andy McMahon for generously providing the *Wnt-8b* probe prior to publication, Jen Lower, Norma Takaesu, and Debbie Pelusi for excellent technical assistance, and Patti Lewko and Mark O'Donnell for expert animal care. These experiments were supported by a grant from the NIH (HD 25208) to E. J. R and by postdoctoral fellowships from the HFSP (I. V.) and EMBO (J. C.).

REFERENCES

Acampora, D., Mazan, S., Lallemand, Y., Avantaggiato, V., Maury, M., Simeone, A. and Brûlet, P. (1995). Forebrain and midbrain regions are deleted in *Otx2*$^{-/-}$ mutants due to a defective anterior neuroectoderm specification during gastrulation. *Development* **121**, 3279-3290.

Ang, S.-L., Conlon, R. A., Jin, O. and Rossant, J. (1994). Positive and negative signals from mesoderm regulate the expression of mouse *Otx2* in ectoderm explants. *Development* **120**, 2979-2989.

Ang, S.-L., Jin, O., Rhinn, M., Daigle, N., Stevenson, L. and Rossant, J. (1996). A targeted mouse *Otx2* mutation leads to severe defects in gastrulation and formation of axial mesoderm and to deletion of rostral brain. *Development* **122**, 243-252.

Ang, S.-L. and Rossant, J. (1993). Anterior mesendoderm induces mouse *Engrailed* genes in explant cultures. *Development* **118**, 139-149.

Ang, S.-L. and Rossant, J. (1994). *HNF-3β* is essential for node and notochord formation in mouse development. *Cell* **78**, 561-574.

Azar, Y. and Eyal-Giladi, H. (1981). Interaction of epiblast and hypoblast in the formation of the primitive streak and the embryonic axis in chick, as revealed by hypoblast-rotation experiments. *J. Embryol. Exp. Morph.* **61**, 133-144.

Barnes, J. D., Crosby, J. L., Jones, C. M., Wright, C. V. E. and Hogan, B. L. M. (1994). Embryonic expression of *Lim-1*, the mouse homolog of *Xenopus XLim-1*, suggests a role in lateral mesoderm differentiation and neurogenesis. *Dev. Biol.* **161**, 168-178.

Beddington, R. S. P. (1994). Induction of a second neural axis by the mouse node. *Development* **120**, 613-620.

Beddington, R. S. P. and Robertson, E. J. (1989). An assessment of the developmental potential of embryonic stem cells in the midgestation embyro. *Development* **105**, 733-737.

Bouwmeester, T., Kim, S.-H., Sasai, Y., Lu, B. and De Robertis, E. M. (1996). Cerberus is a head-inducing secreted factor expressed in the anterior endoderm of Spemann's organizer. *Nature* **382**, 595-601.

Bradley, A. (1987). Production and analysis of chimeric mice. In *Teratocarcinomas and Embryonic Stem Cells: a Practical Approach* (ed. E. J. Robertson), pp. 131-151. Oxford: IRL Press.

Collignon, J., Varlet, I. and Robertson, E. J. (1996). Relationship between asymmetric *nodal* expression and the direction of embryonic turning. *Nature* **381**, 155-158.

Conlon, F. L., Barth, K. S. and Robertson, E. J. (1991). A novel retrovirally-induced embryonic lethal mutation in the mouse; assessment of the developmental fate of ES cells homozygous for the 413.d proviral integration. *Development* **111**, 969-981.

Conlon, F. L. and Beddington, R. (1995). Mouse gastrulation from a frog's perspective. *Seminars in Dev. Biol.* **6**, 249-256.

Conlon, F. L., Lyons, K. M., Takaesu, N., Barth, K. S., Kispert, A., Herrmann, B. and Robertson, E. J. (1994). A primary requirement for *nodal* in the formation and maintenance of the primitive streak in the mouse. *Development* **120**, 1919-1928.

Crossley, P. H. and Martin, G. R. (1995). The mouse *Fgf-8* gene encodes a family of polypeptides and is expressed in regions that direct outgrowth and patterning in the developing embryo. *Development* **121**, 439-451.

Davis, C.A. and Joyner, A. L. (1988). Expression patterns of the homeo box-containing genes *En-1* and *En-2* and the proto-oncogene *int-1* diverge during mouse development. *Genes Dev.* **2**, 1736-1744.

Echelard, Y., Epstein, D. J., St-Jacques, B., Shen, L., Mohler, J., McMahon, J. A. and McMahon, A. P. (1993). Sonic hedgehog, a member of a family of putative signaling molecules, is implicated in the regulation of CNS polarity. *Cell* **75**, 1417-1430.

Friedrich, G. and Soriano, P. (1991). Promoter traps in embryonic stem cells: a genetic screen to identify and mutate developmental genes in mice. *Genes Dev.* **5**, 1513-1523.

Hermesz, E., Mackem, S. and Mahon, K. A. (1996). *Rpx*: a novel anterior-restricted homeobox gene progressively activated in the prechordal plate, anterior neural plate and Rathke's pouch of the mouse. *Development* **122**, 41-52.

Hogan, B., Beddington, R., Costantini, F. and Lacy, E. (1994). *Manipulating the Mouse Embryo: A Laboratory Manual*. New York: Cold Spring Harbor.

Jones, C. M., Kuehn, M. R., Hogan, B. L. M., Smith, J. C. and Wright, C. V. E. (1995). Nodal-related signals induce axial mesoderm and dorsalize mesoderm during gastrulation. *Development* **121**, 3651-3662.

Lawson, K. A., Meneses, J. J. and Pedersen, R. A. (1991). Clonal analysis of epiblast fate during germ layer formation in the mouse embryo. *Development* **113**, 891-911.

Lawson, K. A. and Pedersen, R. A. (1987). Cell fate, morphogenetic movement and population kinetics of embryonic endoderm at the time of germ layer formation in the mouse. *Development* **101**, 627-652.

Lawson, K. A. and Pedersen, R. A. (1992). Clonal analysis of cell fate during gastrulation and early neurulation. In *Postimplantation Development in the Mouse. Ciba Foundation Symposium* (ed. D. J. Chadwick and J. Marsh), 165, pp. 3-26. Chichester: Wiley.

Levin, M., Johnson, R. L., Stern, C. D., Kuehn, M. and Tabin, C. (1995). A molecular pathway determining left-right asymmetry in chick embryogenesis. *Cell* **82**, 803-814.

Lowe, L. A., Supp, D. M., Sampath, K., Yokoyama, T., Wright, C. V. E., Potter, S. S., Overbeek, P. and Kuehn, M. R. (1996). Conserved left-right asymmetry of nodal expression and alterations in murine *situs inversus*. *Nature* **381**, 158-161.

Matsuo, I., Kuratani, S., Kimura, C., Takeda, N. and Aizawa, S. (1995). Mouse *Otx2* functions in the formation and patterning of rostral head. *Genes Dev.* **9**, 2646-2658.

Mitrani, E. and Eyal-Giladi, H. (1981). Hypoblastic cells can form a disk inducing an embryonic axis in the chick epiblast. *Nature* **289**, 800-802.

Monaghan, A. P., Kaestner, K. H., Grau, E. and Schütz, G. (1993). Postimplantation expression patterns indicate a role for the mouse *forkhead*/HNF-3α, β and γ genes in determination of the definitive endoderm, chordamesoderm and neuroectoderm. *Development* **119**, 567-578.

Placzek, M., Jessell, T. M. and Dodd, J. (1993). Induction of floor plate differentiation by contact-dependent, homeogenetic signals. *Development* **117**, 205-218.

Poelmann, R. E. (1981). The head process and the formation of definitive endoderm in the mouse embryo. *Anat. Embryol.* **162**, 41-49.

Robertson, E. J. (1987). Embryo-derived stem cell lines. In *Teratocarcinomas and Embryonic Stem Cells: a Practical Approach* (ed. E. J. Robertson), pp. 71-112. Oxford: IRL Press.

Rosenquist, T. A. and Martin, G. R. (1995). Visceral endoderm-1 (VE-1): an antigen marker that distinguishes anterior from posterior embryonic visceral endoderm in the early post-implantation embryo. *Mech. Dev.* **49**, 117-121.

Shawlot, W. and Behringer, R. R. (1995). Requirement for *Lim1* in head-organizer function. *Nature* **374**, 425-430.

Shimamura, K., Hartigan, D. J., Martinez, S., Puelles, L. and Rubenstein, L. R. (1995). Longitudinal organization of the anterior neural plate and neural tube. *Development* **121**, 3923-3933.

Smith, W. C., McKendry, R., Ribisi, S., Jr. and Harland, R. M. (1995). A *nodal*-related gene defines a physical and functional domain within the Spemann organizer. *Cell* **82**, 37-46.

Sulik, K., Dehart, D. B., Inagaki, T., Vrablic, J. L., Gesteland, K. and Schoenwolf, G. C. (1994). Morphogenesis of the murine node and notochordal plate. *Dev. Dynamics* **201**, 260-278.

Tam, P. P. L. and Beddington, R. S. P. (1992). Establishment and organization of germ layers in the gastrulating mouse embryo. In *Postimplantation Development in the Mouse. Ciba Foundation Symposium* (ed. D. J. Chadwick and J. Marsh), 165, pp. 27-49. Chichester: Wiley.

Thomas, P. and Beddington, R. S. P. (1996). Anterior primitive endoderm may be responsible for patterning the anterior neural plate in the mouse embryo. *Current Biol.* **6**, 1487-1496.

Waddington, C. H. (1933). Induction by the primitive streak and its derivatives in the chick. *J. Exp. Biol.* **10**, 38-46.

Weinstein, D. C., Ruiz i Altaba, A., Chen, W. S., Hoodless, P., Prezioso, V. R., Jessell, T. M. and Darnell, J. E., Jr. (1994). The winged-helix transcription factor *HNF-3β* is required for notochord development in the mouse embryo. *Cell* **78**, 575-588.

Wilkinson, D. G. (1992). Whole-mount in situ hybridization of vertebrate embryos. In *In situ Hybridization: A Practical Approach* (ed. D. G. Wilkinson), pp. 75-83. Oxford: IRL Press.

Wilkinson, D. G., Bhatt, S., Chavrier, P., Bravo, R. and Charnay, P. (1989). Segment-specific expression of a zinc-finger gene in the developing nervous system of the mouse. *Nature* **337**, 461-464.

Zhou, X., Sasaki, H., Lowe, L., Hogan, B. L. M. and Kuehn, M. R. (1993). *Nodal* is a novel TGF-β-like gene expressed in the mouse node during gastrulation. *Nature* **361**, 543-547.

(Accepted 17 December 1996)